Cointegration for Structural Damage Detection Under Environmental Variabilities: An Experimental Study

J. C. Burgos, B. A. Qadri, and M. D. Ulriksen

Abstract An intricacy in vibration-based structural damage detection (VSDD) relates to environmental variabilities (EVs) imposing limitations to the damage detectability. One method that has been put forth to resolve the issue is cointegration. Here, non-stationary vibration features are linearly combined into stationary residuals, which are then employed as damage indices under the assumption that the non-stationarity is governed by environmental variabilities. In the present paper, the feasibility of using cointegration to mitigate environmental variabilities while retaining sensitivity to damage is examined through an experimental study with a steel beam. A temperature-based environmental variability is introduced to the beam by use of a heating cable, while damage is emulated by adding local mass perturbations. The vibration response of the beam in different environmental and structural states is captured and utilized as features in a cointegration-based damage detection scheme. The performance of the scheme is assessed and compared to that of a scheme not accounting for the variability on the basis of the false positive ratio (FPR), the true positive ratio (TPR), and the area under the receiver operating characteristic curve (AUC). The results show that cointegration effectively mitigates the temperature variability and allows for an improved damage detectability compared to that of the scheme without a mitigation strategy.

Keywords Structural health monitoring · Damage detection · Cointegration · Environmental variability · Experimental study

1 Introduction

The objective of vibration-based structural damage detection (VSDD) is to allow for a global assessment of whether or not the structural integrity of the system in question has been compromised. VSDD is conventionally resolved by comparing vibration features extracted from the current, potentially damaged structure to a baseline model composed of the corresponding vibration features extracted from the reference state of the structure [1]. An item that hinders the applicability of VSDD is variability in the environmental parameters (EPs), such as temperature, wind speed, and precipitation [2]. In particular, the dynamic properties of any structure are sensitive to changes in the EPs, thus vibration features exhibit significant changes over time also when no damage is present [3–5].

Numerous supervised and unsupervised learning methods have been proposed to mitigate the influence of environmental variabilities (EVs) in VSDD [1, 6]. The advantage of the unsupervised methods is that they do not require the EPs to be measured, hence making them easier to implement in practice. Cointegration, which is adapted from the field of econometrics [7], is one of these unsupervised methods [8]. The operating assumptions in cointegration-based damage detection are that the EVs render the vibration features non-stationary and that the effects of the EVs and damage do not couple [8]. Hereby, the non-stationary features can be linearly combined to one or multiple stationary residuals in which the non-stationary trends are purged [9].

In the present paper, we evaluate the application feasibility of the VSDD cointegration-based scheme proposed in [6, 10]. In particular, we apply the scheme to mitigate imposed EVs and hence allow for damage detection in a laboratory setting with a cantilevered beam. In the experiment, three damaged states are established by adding three different masses at the top of the beam, while temperature variations are imposed through a heating cable attached to the beam. The performance of the cointegration-based scheme is compared to that of a scheme that does not account for the EVs [11]. The false positive

J. C. Burgos (✉) · B. A. Qadri · M. D. Ulriksen
Department of Energy Technology, Aalborg University, Esbjerg, Denmark

K. Grimmelsman (ed.), *Dynamics of Civil Structures, Volume 2*, Conference Proceedings of the Society for Experimental Mechanics Series, https://doi.org/10.1007/978-3-030-77143-0_6

rate (FPR), the true positive rate (TPR), and the area under the receiver operating characteristic curve (AUC) are used as performance measures for the evaluation.

The paper is organized as follows: a methodology section outlines the explored damage detection schemes, followed by a description of the experimental setup. The damage detection results obtained using the two schemes are reported in the results section, and, lastly, the paper closes with some concluding remarks.

2 Methodology

Let $\boldsymbol{Y}_t \in \mathbb{R}^{F\times m}$ denote a vibration response matrix of a structural system measured through F sensors at a discrete observation $t \in [1,\ N]$. The rows of $\boldsymbol{Y}_t$ contain the F time series of the vibration response, $\boldsymbol{y}_{f,t} \in \mathbb{R}^{1\times m}$, where m is the number of time samples. From the response signals, a set of damage-sensitive vibration features are computed and subsequently used to characterize the state of the structural system as undamaged or damaged by use of some discordance measure.

2.1 Mahalanobis Distance-Based Outlier Analysis of Response Covariances

The covariance matrix of the vibration response matrix $\boldsymbol{Y}_t$ can be established from

$$\forall i \le j \in [1,\ F]: \quad \boldsymbol{\Sigma}_{ij} = \frac{1}{m-1}\sum_{k=1}^{m}(\boldsymbol{Y}_{ik}-\mu_i)(\boldsymbol{Y}_{jk}-\mu_j), \tag{1}$$

where μ_i is the mean of the ith vibration response such

$$\forall i \in [1,\ F]: \quad \mu_i = \frac{1}{m}\sum_{k=1}^{m}\boldsymbol{Y}_{ik}. \tag{2}$$

In this scheme, the feature $\boldsymbol{x}_t$ is constructed from the n unique elements of the covariance matrix $\boldsymbol{\Sigma} \in \mathbb{R}^{F\times F}$, with $n = F(F+1)/2$ since $\boldsymbol{\Sigma} = \boldsymbol{\Sigma}^T$. Thus,

$$\boldsymbol{x}_t = [\boldsymbol{\Sigma}_{11}\ \boldsymbol{\Sigma}_{12}\ \ldots\ \boldsymbol{\Sigma}_{1F}\ \boldsymbol{\Sigma}_{22}\ \boldsymbol{\Sigma}_{23}\ \ldots\ \boldsymbol{\Sigma}_{2F}\ \ldots\ \boldsymbol{\Sigma}_{FF}]^T. \tag{3}$$

The Mahalanobis distance (MD) is used as discordance measure for $\boldsymbol{x}_t$. Let $\boldsymbol{\mu} \in \mathbb{R}^n$ and $\boldsymbol{S} \in \mathbb{R}^{n\times n}$ denote the mean vector and covariance matrix of the features from the training phase in the undamaged/reference structural state, then, in the testing phase, the deviation of $\boldsymbol{x}_t$ from the baseline model is quantified by

$$d^2_{M_t} = (\boldsymbol{x}_t-\boldsymbol{\mu})^T\,\boldsymbol{S}^{-1}\,(\boldsymbol{x}_t-\boldsymbol{\mu}). \tag{4}$$

As such, $d^2_{M_t}$ constitutes the damage index from which inferences regarding the structural state are made. Specifically, if $\mathcal{D}$ is the selected threshold, then $d^2_{M_t} \le \mathcal{D}$ implies that the structure is undamaged, while $d^2_{M_t} > \mathcal{D}$ implies that the structure is damaged.

2.2 Cointegration-Based Scheme

As mentioned introductory, we employ the cointegration-based scheme proposed in [6, 10]. Let $\boldsymbol{c}_{f,t} \in \mathbb{R}^m$ denote the real and imaginary parts of the unique Fourier coefficients of $\boldsymbol{y}_{f,t}$ and take

$$d^2_{M_{f,t}} = \left(\boldsymbol{c}_{f,t}-\boldsymbol{\mu}_f\right)^T \boldsymbol{S}_f{}^{-1}\left(\boldsymbol{c}_{f,t}-\boldsymbol{\mu}_f\right), \tag{5}$$

where $\boldsymbol{\mu}_f \in \mathbb{R}^m$ and $\boldsymbol{S}_f \in \mathbb{R}^{m\times m}$ are the mean vector and covariance matrix of $\boldsymbol{c}_{f,t} \in \mathbb{R}^m$ computed in the training phase for N observations. We gather $d^2_{M_{f,t}}$ in $\boldsymbol{d}^2_{\boldsymbol{M}_f} \in \mathbb{R}^N$ and define the matrix $\boldsymbol{D}^2_{\boldsymbol{M}} = [\boldsymbol{d}^2_{\boldsymbol{M}_1}\ \boldsymbol{d}^2_{\boldsymbol{M}_2}\ \ldots\ \boldsymbol{d}^2_{\boldsymbol{M}_F}]^T \in \mathbb{R}^{F\times N}$. The vector $\boldsymbol{d}^2_{\boldsymbol{M}_t}$, which corresponds to the columns of $\boldsymbol{D}^2_{\boldsymbol{M}}$, is used as feature in the cointegration.

The next step in the scheme is to find a stationary linear combination of the training features to construct a baseline model. To this end, the Johansen cointegration procedure (JCI) [12] is applied. In this procedure, the training features are fitted to the vector error-correction model (VECM)

$$\Delta\boldsymbol{d}^2_{\boldsymbol{M}_t} = \boldsymbol{\Pi}\boldsymbol{d}^2_{\boldsymbol{M}_{t\text{-}1}} + \sum_{i=1}^{k-1} \boldsymbol{C}_i \Delta\boldsymbol{d}^2_{\boldsymbol{M}_{t\text{-}i}} + \boldsymbol{\varepsilon}_t, \tag{6}$$

where $\Delta\boldsymbol{d}^2_{\boldsymbol{M}_t} = \boldsymbol{d}^2_{\boldsymbol{M}_t} - \boldsymbol{d}^2_{\boldsymbol{M}_{t\text{-}1}}$, $\boldsymbol{\varepsilon}_t \sim \mathcal{N}(0,\ \boldsymbol{S})$ is a noise vector, $\boldsymbol{\Pi}$ and $\boldsymbol{C}_i$ are $F \times F$ parameter matrices, and k is the model order (or number of included lags). If the VECM is a true error-correction model and the variables under consideration have the same order of integration (that is, $\Delta\boldsymbol{d}^2_{\boldsymbol{M}_t}$ and $\Delta\boldsymbol{d}^2_{\boldsymbol{M}_{t\text{-}i}}$ are stationary), then $\boldsymbol{\Pi}$ is rank deficient, say of rank r, and can therefore be decomposed as

$$\boldsymbol{\Pi} = \boldsymbol{A}\boldsymbol{B}^T, \tag{7}$$

where $\boldsymbol{A}$, $\boldsymbol{B} \in \mathbb{R}^{F\times r}$ are matrices spanning the column and row spaces of $\boldsymbol{\Pi}$. The column vectors in $\boldsymbol{B}$ can thus be used to project the non-stationary features into stationary residuals. According to the JCI, the vector that gives the most stationary residual is the particular column vector in $\boldsymbol{B}$ associated with the largest eigenvalue [13]. This vector, which we denote $\boldsymbol{\beta}$, is referred to as the cointegrated vector and its corresponding stationary residual, computed as

$$z = \boldsymbol{\beta}^T \boldsymbol{D}^2_{\boldsymbol{M}}, \tag{8}$$

is the cointegrated residual. A set of lags $k_j \in [k_1\ k_2\ \ldots\ k_w]$ is tested in order to find the setting that gives the $\boldsymbol{\beta}$ yielding the most stationary z. The quantification of stationarity is conducted based on the Augmented Dickey-Fuller (ADF) test. The ADF test is employed to test the "degree of stationarity" of each z. In this test, the cointegrated residual is fitted to the model

$$\Delta z_t = \rho z_{t\text{-}1} + \sum_{j=1}^{q-1} b_j \Delta z_{t\text{-}j} + \varepsilon_t, \quad t \in [1,\ N], \tag{9}$$

where q is the number of lags (also referred to as model order) added to ensure that $\varepsilon_t \sim N(0,\ \sigma^2)$. The parameters ρ and b_j in (9) are estimated to fit the model and evaluate the null hypothesis of z being non-stationary. The null hypothesis is evaluated through the test-statistic t_ρ. If t_ρ is lower than the critical value from the Dickey-Fuller tables, z is stationary. The more negative the t_ρ obtained, the more stationary is the z [13].

The results of the ADF depend on the q selected for model (9). For this reason, the ADF of the set of z is performed for a range of $q_i \in [q_1\ q_2\ \ldots\ q_v]$. From each test, the most stationary cointegrated residual and its associated cointegrated vector $\boldsymbol{\beta}_i$ are found. These cointegrated vectors $\boldsymbol{\beta}_i$, $i \in [1,\ v]$, are the ones that give the most stationary cointegrated residuals in the defined ranges of q and k. In this study, the range of values to be used for k is defined according to the procedure described in [14], which is also used for q, thus

$$\boldsymbol{q} = \boldsymbol{k} = \left[3,\ 12\left(\frac{N}{100}\right)^{1/4}\right]. \tag{10}$$

The procedure for finding the set of suitable cointegrated vectors $\boldsymbol{\beta}_i$ within these ranges is summarized in Fig. 1. If the training features are cointegrated, this procedure gives v suitable cointegrated vectors $\boldsymbol{\beta}_i$.

Once $\boldsymbol{\beta}_i$ has been found from the training features, (8) is used to compute the cointegrated residual of each of the features from the testing phase. Let $\mathcal{Z}_L$ and $\mathcal{Z}_U$ denote lower and upper limits, then the structural system in question is labelled as damaged if the testing phase residual is not confined to the interval $[\mathcal{Z}_L, \mathcal{Z}_L]$.

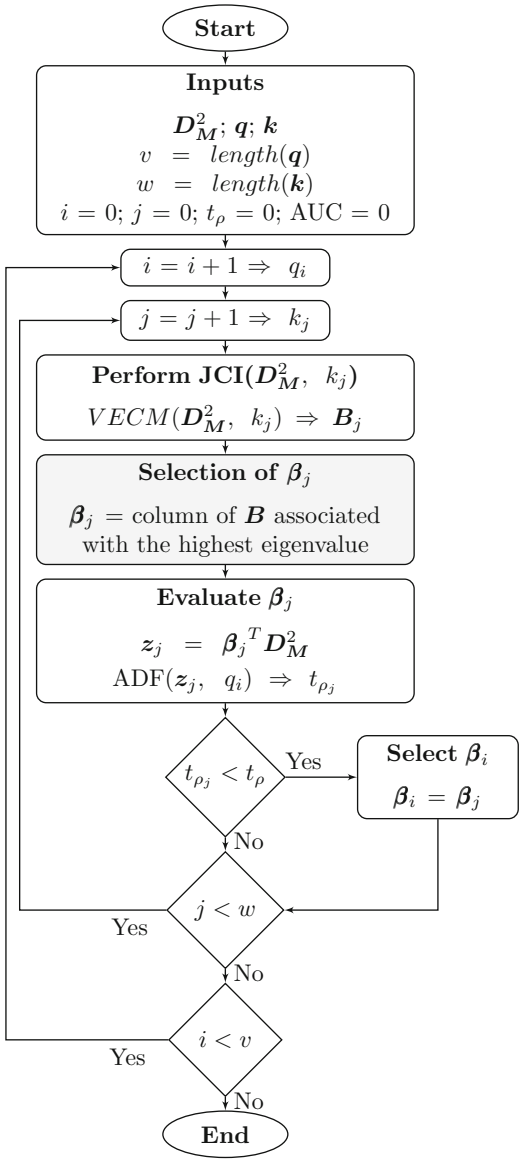

Fig. 1 Procedure to find suitable cointegrated vectors $\boldsymbol{\beta}_i$ from the range of lag values for k and q

3 Laboratory Experiment

The performances of the two VSDD schemes outlined in the methodology section are evaluated experimentally based on a cantilevered steel beam, which is exposed to temperature-based EVs.

3.1 Experimental Setup

The beam, which is depicted in Fig. 2a, is instrumented with nine accelerometers that sample with a frequency of 8192 Hz. In each observation/experimental trial, the accelerometers capture 15 s of the response induced by an impulse load applied to the bottom of the beam. The beam system is analyzed in its reference/undamaged state and in three damaged states, where, as indicated in Fig. 2b, masses of 1, 2.5, and 4.3 g are added in the free end of the beam. Temperature variability is introduced in all structural states by use of a heating cable, which is attached to the beam as seen in Fig. 2c. A thermostat controls the temperature sensed by a NTC thermistor fixed to the beam, and an infrared thermometer is used to measure the temperature.

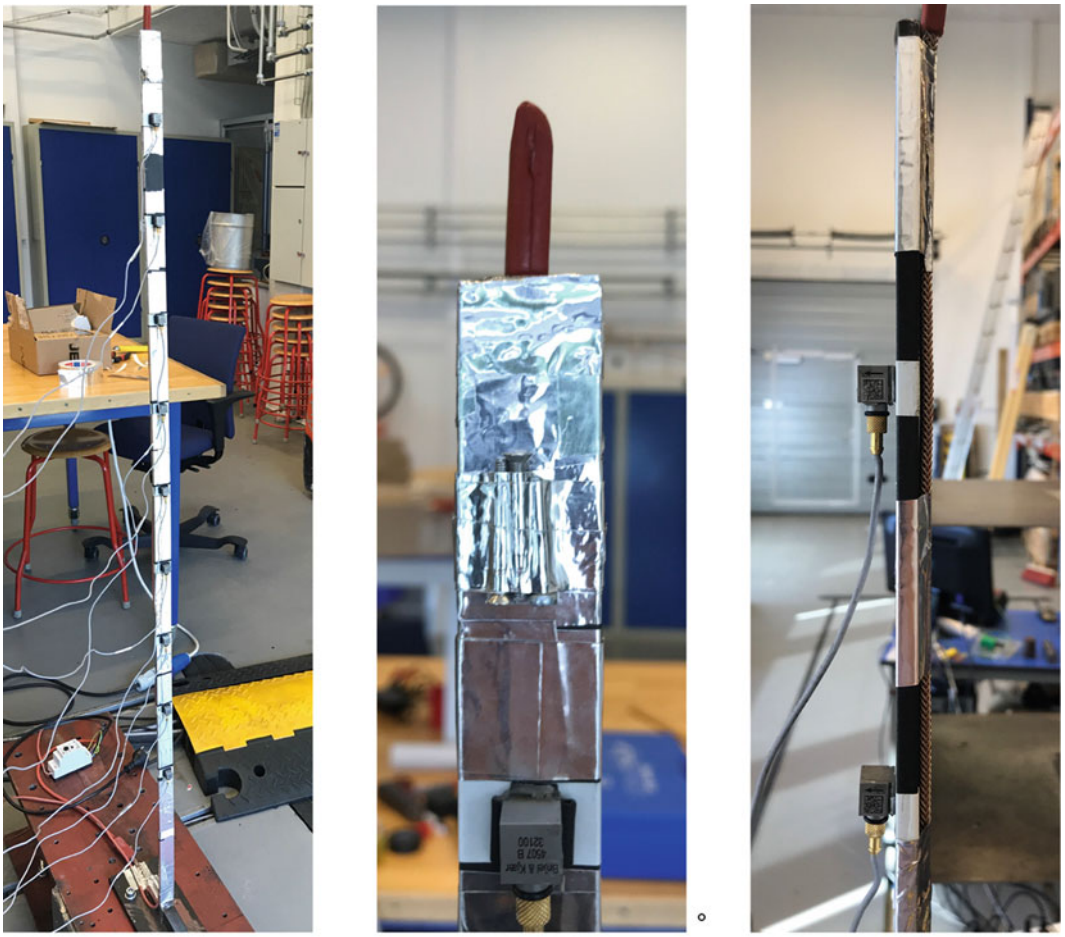

Fig. 2 Cantilevered beam for the laboratory experiment. (**a**) Nine accelerometers mounted on the front of the beam. (**b**) Mass of 4.3 g. Added to the top of the beam to emulate damage. (**c**) Heating cable attached to the back of the beam

The temperature variability is shown in Fig. 3. Evidently, the variability differs for the different structural states, which has been chosen to test the efficiency of the VSDD schemes when some of the EVs are not accounted for in the baseline models.

3.2 Data Acquisition and Feature Extraction

From the 15 s period of available vibration data, an interval of 0.5 s (4096 sample points) is extracted and stored in $\boldsymbol{y}_{f,t} \in \mathbb{R}^{1x4096}$ for further analysis. Training and testing observation sets are obtained from the undamaged state of the beam, and a set of observations is obtained from each of the three damaged states. The features $\boldsymbol{x}_t$ for the MD-based scheme are computed from (3). For the cointegration-based scheme, we plug $\boldsymbol{c}_{f,t} \in \mathbb{R}^{4096}$ into (5) and attain the MDs for each sensor, which are gathered in $\boldsymbol{D}_{\boldsymbol{M}}^2 \in \mathbb{R}^{9\times N}$. The suitable cointegrated vector(s) $\boldsymbol{\beta}_i$ are found from the training features by following the procedure outlined in Fig. 1. From each $\boldsymbol{\beta}_i$, the corresponding cointegrated residual $\boldsymbol{z}_i$ is computed by (8) for the training and testing observations.

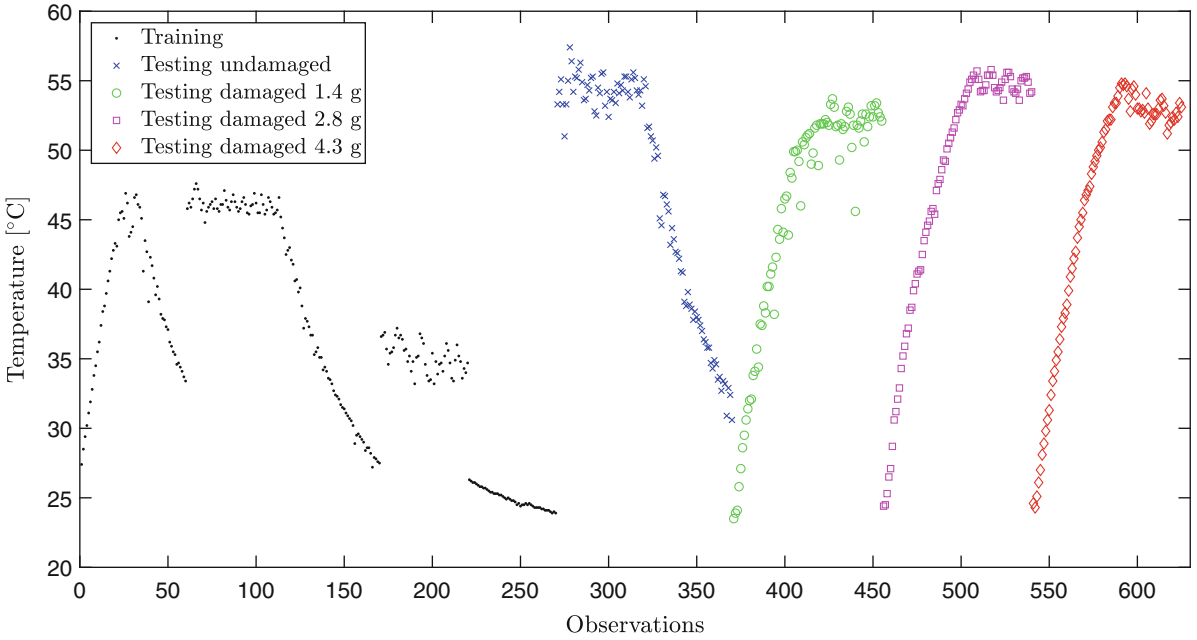

Fig. 3 Temperature field imposed on the beam

4 Results

The baseline models for the VSDD schemes are constructed from $N = 270$ training observations, while 100 observations from the undamaged state and 85 observations from each of the three damaged states are tested against the baseline models. Figure 4a shows the resulting $d^2_{M_t}$ from the MD-based scheme, and the results from the cointegration-based scheme with q =10 and k =10 are displayed in Fig. 4b. In the latter, the mitigation of the influence of the EVs can be clearly appreciated in the testing observations from the undamaged state. To quantify the performance of each scheme, FPRs, TPRs, and AUCs are computed from the damage indices. For the computation of FPRs and TPRs, a threshold of 1% is used in the MD-based scheme, while lower and upper limits of $\pm 1\%$ are used in the cointegration-based scheme. The computed values are summarized in Tables 1 and 2, where it can be seen that the cointegration-based scheme with lag values $q = 10$ and $k = 10$ provides the best performance.

5 Conclusion

The present paper offers a comparative study of two VSDD schemes for detecting mass perturbations in a laboratory beam system exposed to temperature-governed EVs. In particular, the performance of a recently proposed cointegration-based scheme is compared to that of a conventional MD-based outlier analysis scheme that does not account for the EVs. It is found that the cointegration-based scheme allows for a mitigation of the EVs, hence providing an improved damage detection performance compared to that provided by the conventional scheme. It must, however, be noted that the performance of the cointegration-based scheme hinges on a proper selection of the number of lags to include in the VECM and the cointegrated vector(s) to use in the computation of the cointegrated residual(s). To the authors' knowledge, a general procedure for this selection is not available.

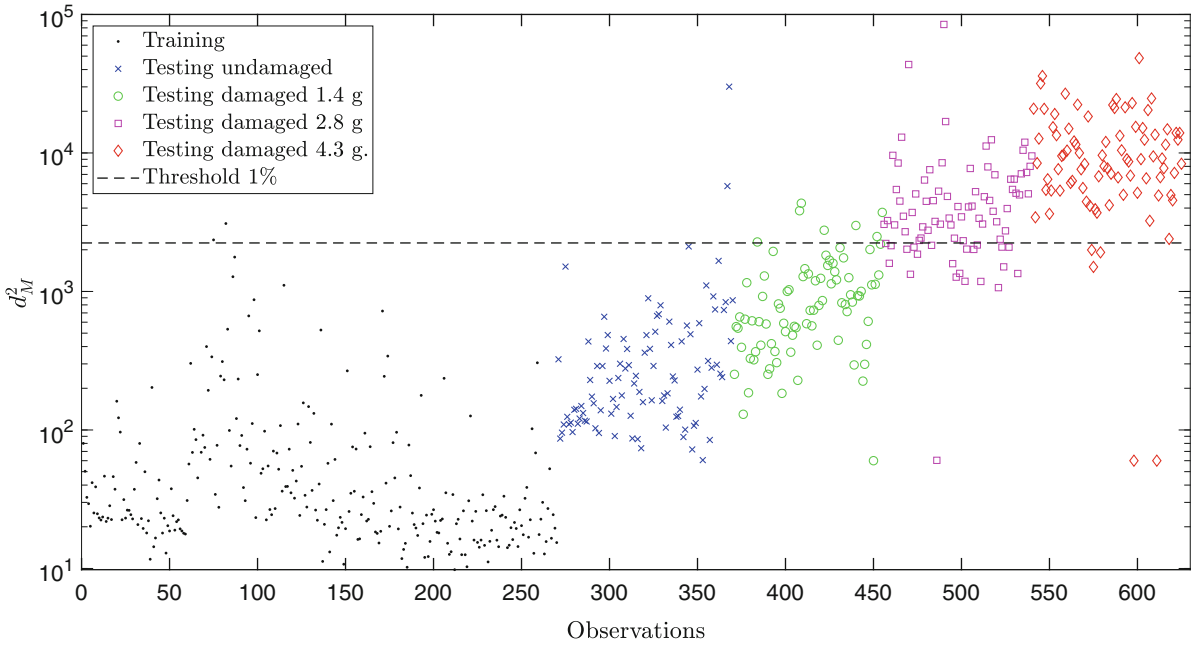

(a)

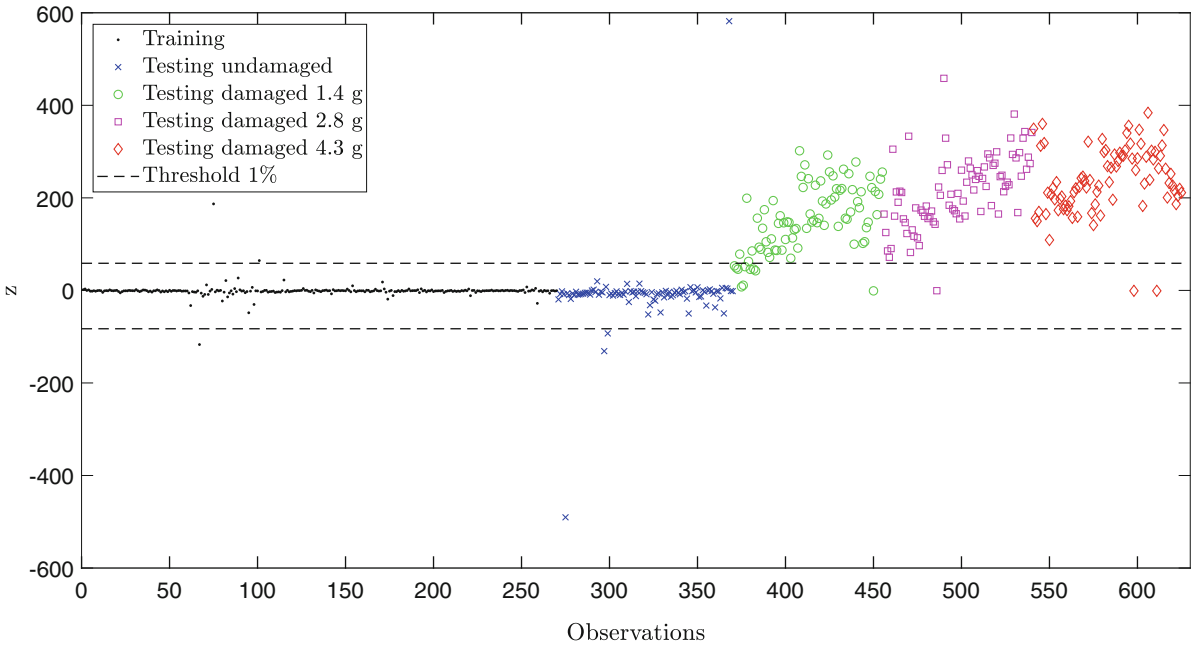

(b)

Fig. 4 Damage detection results. (**a**) MD-based results. (**b**) Cointegration-based results with $q = 10$ and $k = 10$

Table 1 Performance indicators of the MD-based scheme (FPR and TPR for 1% threshold)

AUC	FPR (%)	TPR (%)
0.9193	2.00	58.82

Table 2 Performance indicators of the cointegration-based scheme (FPR and TPR for limits of ±1%)

q	k	AUC	FPR (%)	TPR (%)
3	7	0.9282	3.00	29.80
4	12	0.9496	4.00	71.37
5	10	0.9456	4.00	75.46
6	11	0.9422	5.00	77.25
7	8	0.9161	2.00	28.62
8	8	0.9161	2.00	28.62
9	8	0.9161	2.00	28.62
10	10	0.9841	4.00	92.15
11	8	0.9161	2.00	28.62
12	11	0.9422	5.00	77.25
13	11	0.9422	5.00	77.25
14	12	0.9496	4.00	71.37
15	8	0.9161	2.00	28.62

References

1. Farrar, C.R., Worden, K.: Structural Health Monitoring: A Machine Learning Perspective, 1st edn. Wiley, Hoboken, NJ (2013)
2. Ulriksen, M.D.: Damage localization for structural health monitoring: an exploration of three new vibration-based schemes, Ph.D. thesis, Aalborg University, Aalborg (2018)
3. Wahab, M.A., Roeck, G.D.: Effect of temperature on dynamic system parameters of a highway bridge. Struct. Eng. Int. **7**(4), 266–270 (1997). https://doi.org/10.2749/101686697780494563
4. Peeters, B., De Roeck, G.: One-year monitoring of the z24-bridge: environmental effects versus damage events. Earthquake Eng. Struct. Dynam. **30**(2), 149–171 (2001). http://dx.doi.org/10.1002/1096-9845(200102)30:2<149::AID-EQE1>3.0.CO;2-Z
5. Augustyn, D., Smolka, U., Tygesen, U.T., Ulriksen, M.D., Sørensen, J.D.: Data-driven model updating of an offshore wind jacket substructure. Appl. Ocean Res. **104**, 102366 (2020). http://dx.doi.org/10.1016/j.apor.2020.102366
6. Qadri, B.A., Avendaño-Valencia, L.D., Hooghoudt, J.-O., Tcherniak, D., Ulriksen, M.D.: Removal of environmental and operational effects in damage detection: a comparative study with an operating wind turbine. Struct. Health Monit. (submitted)
7. Engle, R., Granger, C.: Co-integration and error correction: representation, estimation, and testing. Econometrica **55**(2), 251–276 (1987)
8. Cross, E.J., Worden, K., Chen, Q.: Cointegration: a novel approach for the removal of environmental trends in structural health monitoring data. Proc. R. Soc. A: Math. Phys. Eng. Sci. **467**(2133), 2712–2732 (2011). https://doi.org/10.1098/rspa.2011.0023
9. Cross, E.J., Worden, K., Sturgeon, R.J., Chen, Q.: A tutorial on cointegration for engineers—a tool for non-stationary time series analysis. In: Proceedings of the 10th International Conference on Recent Advances in Structural Dynamics, Southampton (2010), pp. 12–14
10. Qadri, B.A., Avendaño-Valencia, L.D., Hooghoudt, J.-O., Ulriksen, M.D.: A cointegration-based scheme for damage detection under environmental and operational variability. Struct. Health Monit. (in preparation)
11. Tcherniak, D., Mølgaard, L.L.: Active vibration-based structural health monitoring system for wind turbine blade: demonstration on an operating Vestas V27 wind turbine. Struct. Health Monit. **16**(5), 536–550 (2017)
12. Johansen, S.: Statistical analysis of cointegration vectors. J. Econ. Dynam. Control **12**(2), 231–254 (1988). https://doi.org/10.1016/0165-1889(88)90041-3
13. Cross, E.J., Worden, K., Chen, Q.: Cointegration: a novel approach for the removal of environmental trends in structural health monitoring data. Proc. R. Soc. A Math. Phys. Eng. Sci. **467**(2133), 2712–2732 (2011)
14. Dao, P.B., Staszewski, W.J., Klepka, A.: Stationarity-based approach for the selection of lag length in cointegration analysis used for structural damage detection. Comput.-Aided Civil Infrastr. Eng. **32**(2), 138–153 (2017)